Tomo PTV using 3D Scanning Illumination and Telecentric Imaging

J. Kitzhofer[1], C. Brücker[1] and O. Pust[2]

[1]Institut für Mechanik und Fluiddynamik, Professur für Strömungsmechanik und Strömungsmaschinen,
TU Bergakademie Freiberg, 09596, GERMANY
Jens.Kitzhofer@imfd.tu-freiberg.de

[2]Dantec Dynamics A/S, DK-2740 Skovlunde, DENMARK

ABSTRACT

The article discusses the tomographic reconstruction of particles for the flow visualisation technique PTV (Particle Tracking Velocimetry) and its application on the real flow of a vortex ring using 3D scanning illumination and telecentric imaging. In standard 3D PTV an increasing number density of particles increases the problem of stereo-matching and overlapping particle images limiting the resolution for a three camera set-up to 0.005 ppp (particles per pixel)[5]. Therefore, in classical 3D PTV the maximum number of observable trajectories is limited to the order of 10^3 in a typical cubic volume. This number can be increased by developments like Scanning PTV [5,7]. However, the mentioned limitations still exist. Tomo PTV in combination with a scanning illumination overcomes these limitations within at least a doubling of the spatial resolution of every single scanned volume. The model flow to determine the measurement method of Tomo PTV described herein is a vortex ring.

1. INTRODUCTION

The investigation of flow fields is usually performed within an Eulerian framework. For the analysis of turbulent flows the Lagrangian frame gives additional important information about turbulent mixing, dispersion etc. This requires the reconstruction of long Lagrangian trajectories with a high spatial resolution. In standard 3D PTV methods the epipolar geometry is used to detect corresponding particle images between different camera views after the localisation of the 2D centroid positions. The tracking of the particles is done either in 2D or in 3D or as a combination of both. The problem of stereo-matching and overlapping particle images limit the maximum number of linkable particles from one frame to the other frame to a number of 0.005 ppp (particles per pixel)[5]. In Tomo PTV the tracking is done in 3D space after the determination of the 3D centroid positions of the particles in space. The tomographic reconstruction of the particles is performed as a combination of the epipolar geometry and a multiplication of gray-values of corresponding pixels in the different camera views [4]. This is possible due to the telecentric imaging resulting in a parallel projection for the observed volume. Each pixel value in one camera occupied by a particle is multiplied with all pixel values along the corresponding epipolar line in the other camera. Thus gray-value-weighted particles are reconstructed at defined voxel positions. The by-product of tomographic reconstructions is the reconstruction of ghost particles [1]. In particle tracking methods it is sufficient to detect and to delete ghost particles for not building false particle paths. Different detection criteria are necessary to decrease the number of ghost particles [4]. The strongest decrease is achieved by the use of a multi-camera-setup. Furthermore ghost particles can be detected by a size based criterion, because ghost particles often appear as a particle artefact [7]. Beside the fact that a scanning illumination can increase the spatial resolution of standard PTV [2], the scanning illumination helps to detect ghost particles. Reconstructed particles appearing in a region without illumination are identified to be ghost particles. The ghost particles appearing within the illuminated sheet are detected by the particle tracking method itself. The tracking is done with the 4-frame method after performing the 3D particle reconstruction and the following 3D centroid localization in the object space. A condition for the detection of ghost trajectories is the smoothness of a trajectory. Ghost trajectories are blinking or are too short to build up the true path of a trajectory.

2. TOMOGRAPHIC RECONSTRUCTION

2.1 Principle

A mathematical model for a stereoscopic camera setup is given by the epipolar geometry. It describes, that a point, which is found in one camera, has to be along a line in the second camera. Mathematically the relation between both cameras is described by the fundamental matrix F. The relation of a 2D image position in camera one to the position in camera two is called epipolar equation resulting in a line in camera two called epipolar line. In the context of calibration, the fundamental matrix has to be evaluated for each combination of the cameras.

Once the fundamental matrix is determined, gray value weighted particles can be reconstructed at defined voxel positions. The epipolar line for each pixel in one camera occupied by a gray value larger than zero is determined. The position of the voxel element is defined by the pixel position in camera one and by the position along the epipolar line. The gray value of the voxel element is calculated by a multiplication of gray values of corresponding pixels in both image views (fig.1).

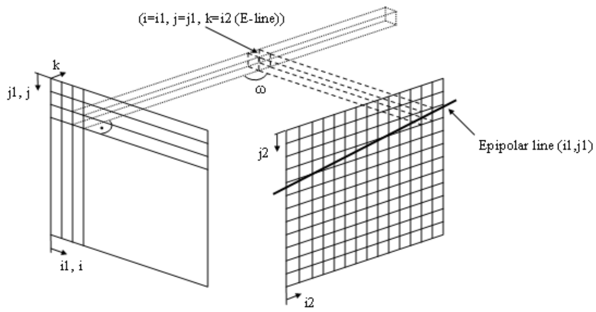

Figure 1: Tomographic reconstruction

If more than two cameras are used to reconstruct the particles in the measured volume, the reconstructed volumes for each combination of cameras have to be multiplied [4].

The investigations in this article are performed for a three camera set-up with scanning illumination. Ten cinematic light sheets with a thickness of 10 mm illuminate the measured volume. The light sheets have an overlap of 1 mm. The tomographic reconstruction of the particles is performed for each light sheet. After the 3D centroid determination, the reconstructed light sheet volumes are combined. In the overlapping regions the same particles are reconstructed twice. The accuracy of the twice reconstructed particles is 1/10 pixel, resulting in a simple nearest neighbour comparison to find twice reconstructed particles.

2.2 Detection of Ghost Particles
The first detection criterion is the combination of reconstructed volumes due to a multi-camera set-up. Figure 2 shows the number of reconstructed particles as a function of the real number of particles for a two camera set-up and a three camera set-up. The dataset is generated with synthetic particles in a defined voxel space. The particle size is homogenous (7 voxel). The red line shows the results for a two camera set-up. With increasing number of real particles the number of reconstructed particles increases rapidly. A three camera set-up (green line) can strongly decrease the number of ghost particles. 20 % of the reconstructed particles are ghost particles for 0.01 ppp.

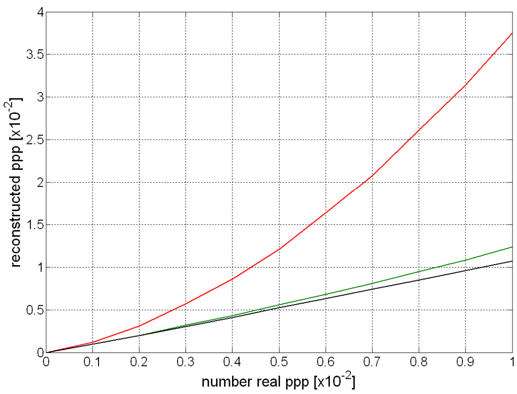

Figure 2: Reconstructed particles as a function of real particles for a 2-camera setup (red line), a 3-camera setup (green line) and the 3-camera setup with size based criterion (black line)

The second detection criterion is called size based criterion. Ghost particles appear as a kind of artefact of particles [7]. This means that ghost particles don't have the same size as reconstructed real particles. A simple threshold is chosen to delete the particles, which are too small to be real particles. In the present synthetic dataset the threshold is set to 4 voxel resulting in a reduction of 14 % for 0.01 ppp in comparison with the 3-camera setup.
The third implemented criterion is the detection of ghost particles due to the light sheet thickness. If a particle is reconstructed at a position in space, where has been no illumination, the reconstructed particle is deleted as will be described in section 4.

3. PARTICLE TRACKING

3.1 Determination of Centroid Positions
Ouellette et al. [6] compared several algorithms for determining the centers of particles. The Gaussian fitting delivered best results due to sub-pixel accuracy, speed and robustness to noise. The accuracy for determining the centers is estimated with a synthetic dataset. Particles (7 voxel) are randomly distributed in voxel space and parallel projected onto the synthetic image planes. Afterwards the particles are reconstructed as described in section 2. By comparison with the known 3D particle position the accuracy of the determination of the particle positions can be evaluated. The accuracy σ is defined as the difference between the estimated position and the true position of a particle. The accuracy σ_i in direction i is 0.12 pix, σ_j in direction j is 0.02 pix and σ_k in direction along the epipolar line is 0.15 pix for the 3-camera set-up.

3.2 Tracking Algorithm
Ouellette et al. [6] tested the quality of several 3D tracking algorithms. The quality of the 4-frame method (Minimum Change in Acceleration) outperformed the other tested algorithms like Nearest Neighbour or 3 frame algorithm. An upgrade for the 4-frame method is achieved herein due to the tomographic reconstruction. As the size of the particles is known in 3D space, ambiguities can be decreased. The quality function for possible linked particles from one frame to the next frame reads:

$$\Phi^{t}_{ij,size} = \left\| \mathrm{N}^{t+1}_{ij} - \mathrm{N}^{t}_{ij} \right\| \tag{1}$$

N^t indicates the number of occupied voxel of a particle at frame t and N^{t+1} the number of occupied voxel of a particle at frame t+1. The particle with the smallest change in size is chosen for the trajectory.
If this criterion provides no solution, the 3D intensity distribution of the possible candidates (t+1) is compared with the 3D intensity distribution of the particle already being part of the trajectory (t). The one with the best fit is chosen.

$$\Phi^{t}_{ij,\mathrm{int}} = \left\| \left(\frac{\sum_N I_{N,ij}}{\max(I_N)} \right)^{t+1} - \left(\frac{\sum_N I_{N,ij}}{\max(I_N)} \right)^{t} \right\| \tag{2}$$

3.3 Detection of Ghost Trajectories
The following two criteria are grouped in the detection of short and long ghost trajectories. Figure 3 shows a typical result for a tomographic reconstructed trajectory and its surroundings in case of the experimental setup that will be described in section 4.

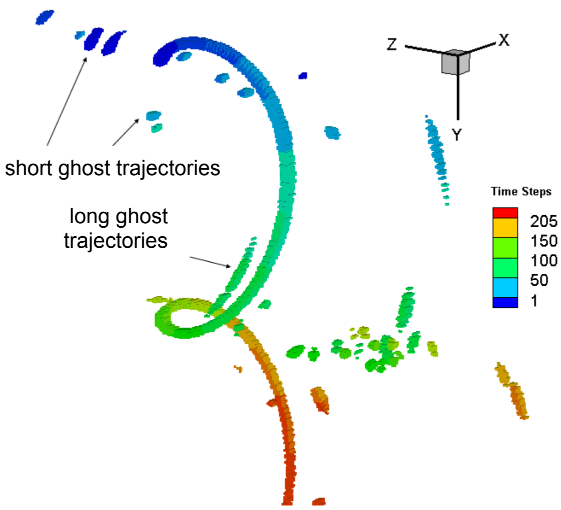

Figure 3: Reconstructed trajectory and environment

The criteria for short ghost trajectories can be interpreted as a kind of save threshold. Most of the ghost trajectories are of small lengths up to three frames. Particle paths existing for only three frames don't yield much information for a fluid mechanical interpretation. Thus a cut off is made, which has to be chosen carefully not to delete true particle paths.

For the detection of long ghost trajectories, a first guess tests the similarities of trajectories in 3D space. This checks frame identity, speed, direction and change in direction. Trajectories fitting these conditions are compared. Long parallel ghost trajectories have a characteristic blinking. The particle path has breaks. Moreover, characteristic for this kind of ghost trajectory is the size of the particle building a trajectory. The particle size in true trajectories is nearly constant. The particle size of ghost trajectories building a path changes while moving along the particle path [4]. Usually the particle appears small sized in the beginning, grows up to a maximum size and shrinks until appearing no more in space. If these criteria fit a selected trajectory, the trajectory is a ghost trajectory and is deleted.

4. EXPERIMENT

4.1 Experimental Set-up

The experimental set-up is shown in figure 4. The laser beam of a continuous Argon-Ion laser (a) Coherent Innova 70 (2 W) passes an optical lens system (b) to adjust the desired thickness of the light sheets. The rotating mirror drum (c) reflects the laser beam into the direction of the observed volume and generates successively 10 parallel light sheet planes with a thickness of 10 mm (f) [3]. The studied flow is a vortex ring travelling in an octagonal glass tank (e) filled with water. The vortex is generated at the exit of a piston tube with a diameter of 50 mm (g). The neutrally buoyant seeding particles (100 microns) are injected into the center of the vortex generator. The particle images are recorded with a three camera system consisting of digital high speed cameras Photron APX RS with a resolution of 1024 x 1024 Pixel² and an angular displacement of 45°, -45° and 90°. The cameras are equipped with telecentric lenses at f-number 16 resulting in a parallel projection for the observed volume. The side of the octagon opposite to the entrance side for the laser is covered with a light absorbing mat that reduces stray reflections. This is also valid for the faces opposite the cameras, thus giving a perfectly black background. The experiments are performed with a recording rate of 1000 frames/s. Using 10 scanning planes results in a separation time of 10 ms for each subsequent illumination of one scan plane. The image size of the cameras and the light sheet thickness define the measured volume, resulting in about 90 x 90 x 90 mm³.

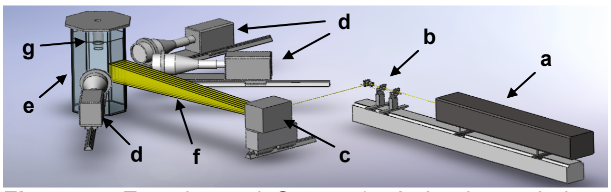

Figure 4: Experimental Set-up (a Ar-Ion-laser, b lens system, c rotating mirror drum, d high speed camera, e octagon, f light sheets, g vortex generator)

4.2 Results

4.2.1 Tomographic Reconstruction

The tomographic reconstruction of one scanning light sheet in the middle of the vortex ring for one single frame is shown in figure 5. Figure 5a shows an isometric view of the vortex ring. The data presented is evaluated with the 3-camera setup and the size based criterion. The shape of the vortex ring is clearly recognizable. Figure 5b shows the vortex ring in the top view. The outer borders of the scanning light sheet are illustrated with red lines. Moreover the particles appearing outside the illuminated light sheet are marked red. These particles are identified to be ghost particles and can be deleted for further investigations.

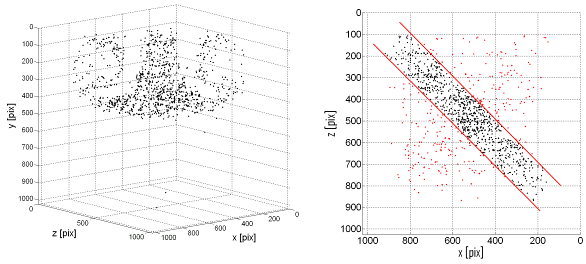

Figure 5: a) Isometric view b) Top view of one light sheet in the middle of the vortex ring

The connection of the ten scanning light sheets for one total scan is shown in figure 6. Every different coloured light sheet means a successive scan. The circled shape of the vortex ring is recognizable.

The overlapping area between the fifth and the sixth light sheet is marked with blue lines. Inside the overlapping area particles are marked with yellow dots. These particles are reconstructed in both light sheets, found by the nearest neighbour comparison. As described above, the accuracy is 1/10 pixel.

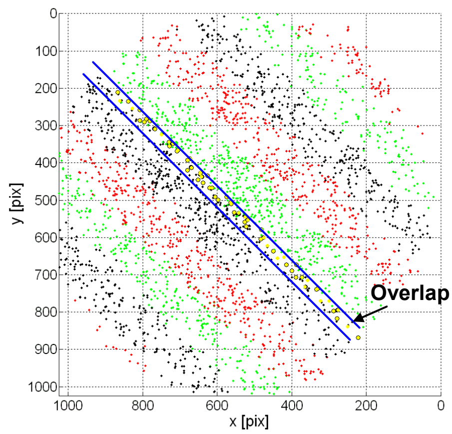

Figure 6: Top view of the connection of the scanning light sheets for one total scan

4.2.2 Particle Tracking

The result for the 3D trajectories of one scanning light sheet in the middle of the vortex is shown in figure 7. The cut off of the trajectories on the right side of the vortex ring results from the viewing field of the third camera. This part of the vortex could not be observed by the third camera. Nevertheless, the shape is clearly recognizable. The reason for the high magnitude in absolute velocity in the inner part of the axis of rotation is that the induced velocity of the vortex ring is superimposed with the translational velocity of the vortex ring. This is in well agreement with the fluid mechanical characteristics of a vortex ring.

At the end of the width of the light sheet appear trajectories, which have a sudden cut off. These trajectories continue in the next light sheet. Figure 8 shows the connection of the ten scanning planes for a moving observer as a function of absolute velocity. A cut between the light sheets is not recognisable.

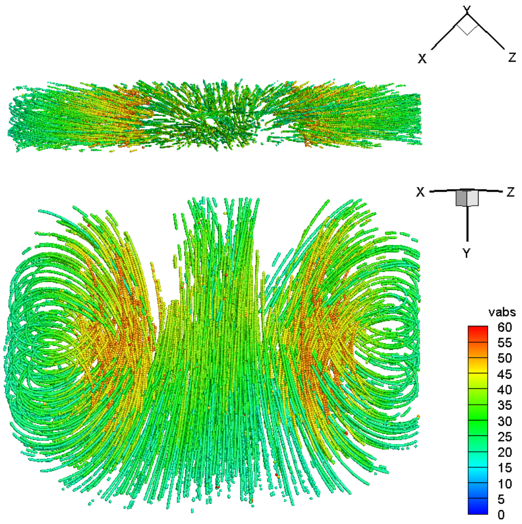

Figure 7: Reconstructed trajectories for one scanning light sheet as a function of velocity [mm/s] **a)** top view **b)** isometric view

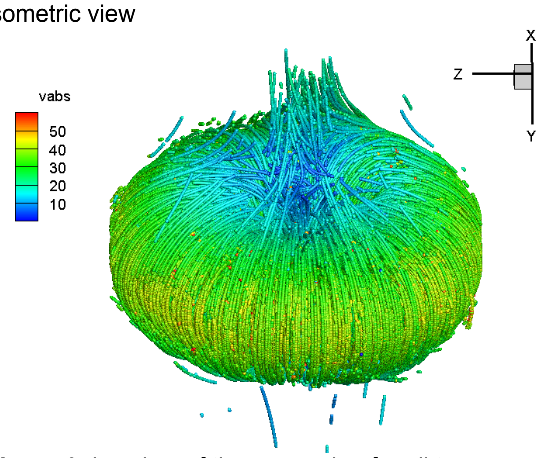

Figure 8: Iso view of the vortex ring for all ten scanning planes as a function of absolute velocity [mm/s]

The accuracy of the calculated velocity is estimated by the standard deviation. Assuming that the vortex ring is in the laminar phase, the total standard deviation of all reconstructed trajectories σ_{vx} in x-direction is 2.42 mm/s, σ_{vy} in y-direction is 1.66 mm/s, σ_{vz} in z-direction is 2.32 mm/s and σ_{vabs} for the magnitude in velocity is 2.16mm/s.
Table 1 describes the statistics of Tomo PTV with a scanning illumination for the vortex ring experiment. About the half of the observed volume was seeded with particles. In all scanning planes the median number of links, meaning a particle observable and linkable for two time steps, is 3000. If the whole volume is seeded with particles, the links can be increased and then calculates to 6500. The efficiency of Tomo PTV with a scanning illumination becomes clear by the 18000 trajectories, which could be reconstructed for more than 10 time steps.

5. CONCLUSION

Tomographic Particle Tracking Velocimetry can increase the spatial resolution of determined trajectories about a factor two in comparison with standard PTV. Moreover the scanning illumination increases the number of trajectories about the factor of number light sheets. Nevertheless, the number of linkable particles is no more defined by the problem of stereo matching or overlapping particles, but by the detection of ghost particles and the ratio of distance between particles and median particle displacement.
The telecentric imaging simplifies the reconstruction algorithms and increases the size of the measured volume about the depth of focus of the telecentric lenses. As well as commonly used reconstruction algorithms like for example MART [1], the processing time of the reconstruction algorithm is long. Further developments have to optimize the processing time.

Observed Volume	700 cm³
Seeded Volume	320 cm³
Light Sheets	10
Light Sheet thickness	1 cm
Light Sheet Overlap	0,1 cm
Median particle displacement	5 pixel
Median Number of Links (Light Sheet in the middle)	1050
Median Number of Links (All Light Sheets)	3000
Calculated Number of Links (Observed Volume)	6500
Total Number of Trajectories (All Light Sheets)	18000

Table 1: Statistics of Scanning Tomo PTV in application of the vortex ring

ACKNOWLEDGMENTS

The authors thank Prof. Maas for the discussions and the brainstorming about the calibration procedure and the particle tracking. Moreover, the authors thank Dantec Dynamics for the support of the hardware equipment.

REFERENCES

[1] Elsinga G.E. (2008) Tomographic Particle Image Velocimetry, *Ph.D. Thesis,* Department of Aerospace Engineering, Delft University of Technology

[2] Hoyer, K., Holzner, M., Lüthi, B., Guala, M., Liberzon, M., Kinzelbach, W. (2005) 3D Scanning Particle Tracking Velocimetry, Experiments in Fluids 39, 923-934

[3] Kitzhofer, J., Kirmse, C., Brücker, Ch. (2009) 3D Scanning Particle Tracking Velocimetry by using High Speed Digital Cameras and Telecentric Lenses, Notes on Numerical Fluid Mechanics, Springer Verlag

[4] Kitzhofer, J., Brücker, Ch. (2009) Tomographic Particle Tracking Velocimetry, submitted to Experiments in Fluids

[5] Maas H.G. (1992) Digitale Photogrammetrie in der dreidimensionalen Strömungsmesstechnik, *Ph.D. Thesis*, ETH Zürich

[6] Ouelette, N.T., Xu, H., Bodenschatz, E., (2006) A quantitative study of three-dimensional Lagrangian particle tracking algorithms, Experiments in Fluids 40, 301-313

[7] Putze, T. (2008) Geometrische und stochastische Modelle zur Optimierung der Leistungsfähigkeit des 3D PTV, *Ph.D. Thesis,* Fakultät Forst-, Geo- und Hydrowissenschaften, Dresden University of Technology